Plan of Talk

- X-ray studies of radio jets lobes and hot spots in radio galaxies and quasars.
- Influence of radio ejecta on gas in clusters of galaxies
- The random orientation of radio jets in active disk (i.e. Seyfert) galaxies.
- Jets in low luminosity active galactic nuclei (LLAGN) dominate electromag. luminosity from accretion onto SMBH.

X-RAY EMISSION PROCESSES IN RADIO JETS AND HOT SPOTS

- **THERMAL**

Collisionally ionized (10^{7-8}K)
Photoionized (several $\times$ 10^4 - several $\times$ 10^5K)
Is it observed? - No (1 possible exception)

- **INVERSE COMPTON SCATTERING**

$e + \nu_0 \rightarrow e + \nu_1$
$\nu_1 \sim \gamma^2 \nu_0$
If $n(\gamma) = n_{e0}\gamma^{-p}$, $\alpha_C = \alpha_S = (p-1)/2$
Is it observed? - Yes
What do we learn? Magnetic field strength plus constraints on Γ and θ if bulk relativistic motion is present

- **SYNCHROTRON RADIATION**

$\nu_1 \sim \gamma^2 \nu_g$
Need $\gamma \sim 10^{7-8}$ for X-rays
Is it observed? - Yes
What do we learn? Cosmic ray acceleration processes work *in situ* to these γ's and, if protons of similar γ are present, $E_{cr} \sim 10^{16-17}$ eV (cf. max energy of cosmic rays observed is $\sim 10^{21}$)

INVERSE COMPTON SCATTERING. SOURCES OF PHOTONS.

- The synchrotron radiation itself (synchrotron self-Compton radiation - SSC.)
- The cosmic microwave background radiation (external Compton, EC). Note:
  1) $\epsilon_{CB} = \epsilon_{CB0}\ (1+z)^4$, so expect an increase of L_X with z
  2) $\gamma \sim 1{,}000$ (typically meter wave radio synchrotron electrons)
- The galaxy starlight. Note: Very low energy cosmic rays needed ($\gamma \sim 20$), not observable as radio synchrotron.
- Radiation from the active nucleus, probably beamed along the radio axis. Note:
  1. Radiation is probably dominated by IR, so $\gamma \sim 100$ - 300 (below normal radio band)
  2) Angle dependence of IC scattering $\Rightarrow$ more distant lobe should be somewhat (depending on θ) more luminous (Brunetti et al. 1997)

BULK RELATIVISTIC MOTION.

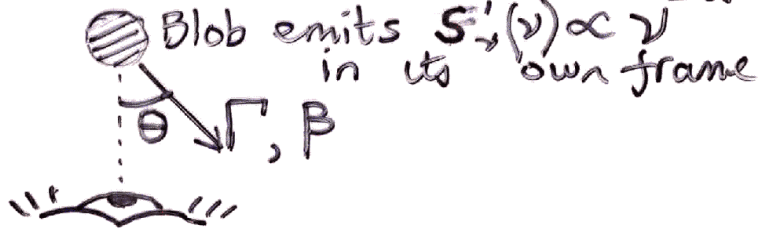

- **Effect depends on Doppler factor:**

$\delta = [\Gamma(1 - \beta\cos\theta)]^{-1}$

where Γ = Lorentz factor, $\beta = v_{bulk}/c$, θ = angle between velocity vector and line of sight.

Note: $\delta_{max} = 1/\sin\theta$, and is achieved when $\sin\theta = 1/\Gamma$.

1. Radiation isotropic in blob frame (usually assumed for synchrotron and SSC radiation)

$S_\nu(\nu) \propto \delta^{3+\alpha} S'_\nu(\nu)$.

If $S_{\nu,SSC}$ too weak, must increase N_{e0} and (equivalently) decrease B ($B \propto \delta^{-(3+\alpha)/(1+\alpha)}$).

2. Radiation isotropic in (e.g.) Hubble frame (as applies to cosmic background and approximately to galaxy starlight)

$S_\nu(\nu) \propto \delta^{4+2\alpha} S'_\nu(\nu)$ (Dermer 1995).

So $S_{\nu,EC}/S_{\nu,synch} \propto \delta^{1+\alpha} S'_\nu(\nu)$.

Thus can get large boost of $S_{\nu,EC}$ if $\delta > 1$. Expect this effect to be important for jets with small θ (BL Lacs, blazars).

JETS OBSERVED WITH CHANDRA

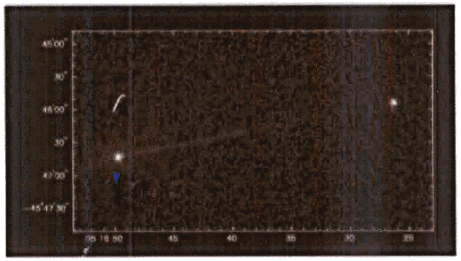

Pictor A (Wilson, Young & Shopbell 2001, ApJ, 547, 740)

100 kpc PICTOR A

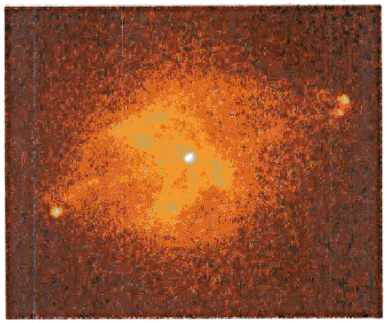

100 kpc

Cygnus A (Wilson, Young & Shopbell 2001, ApJ, 544, L27)

CYGNUS A

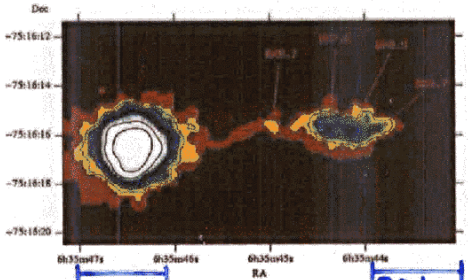

PKS 0637-752 (Chartas et al. 2000, ApJ, 542, 655)

30 kpc

PKS 0637-752

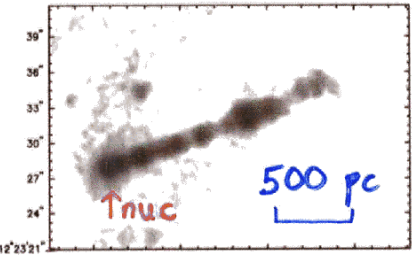

M 87 (Wilson & Yang 2002, ApJ, 568, 133)

M87

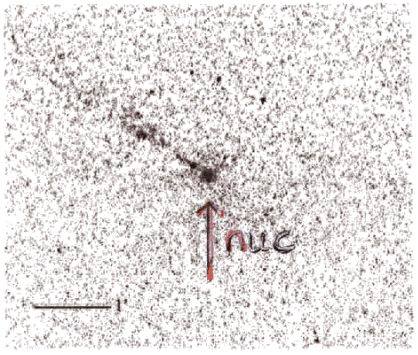

Centaurus A (Kraft et al. 2000, ApJ, 531, L9)

CENTAURUS A

1 kpc

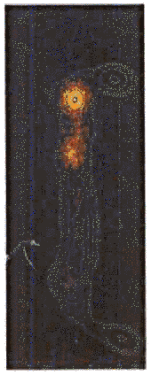

20 kpc

3C 273 (Marshall et al. 2001, ApJ, 549, L167)

3C 273

New (≃ 200 ks) Chandra obsn of Cyg A, with radio contours

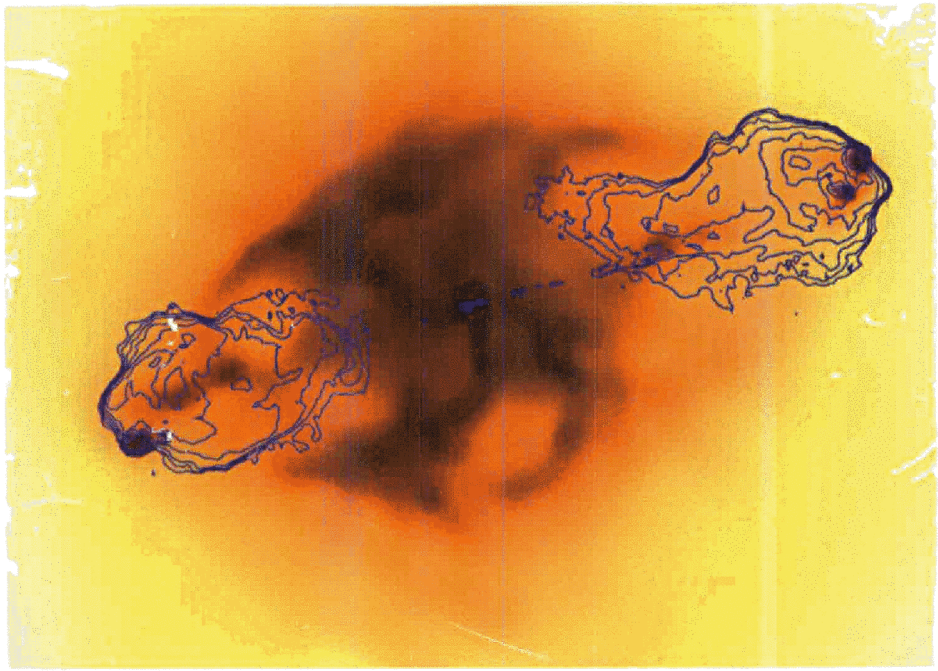

A. J. Young, S. Heinz, C. Carizares, A. S. Wilson

Cygnus A – western hot spots

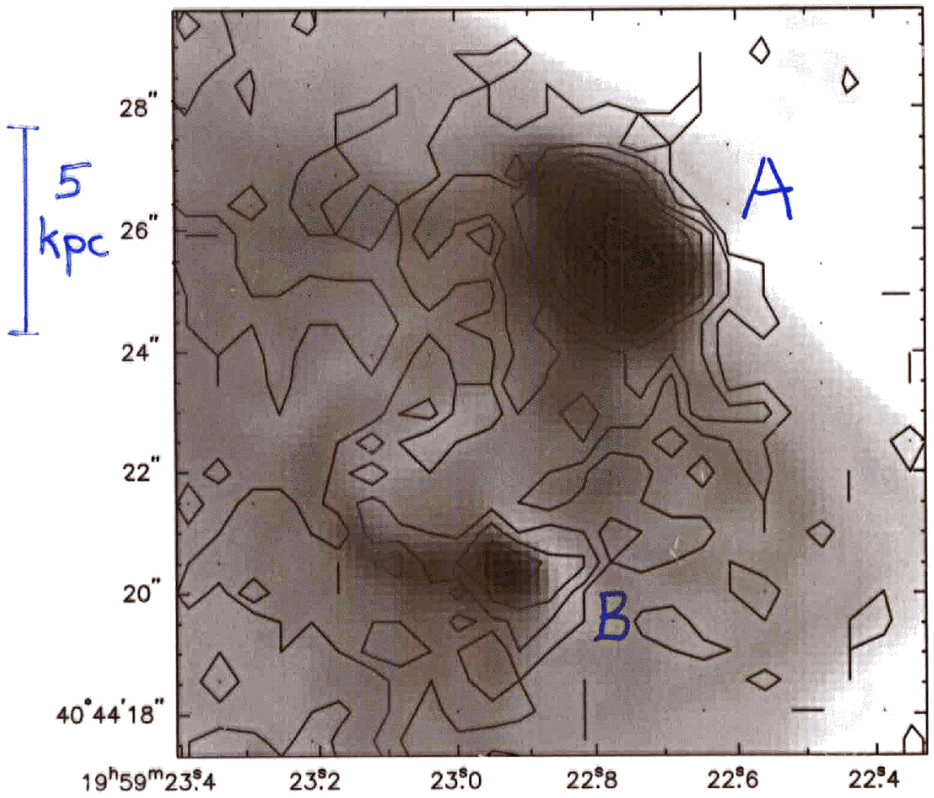

Contours – X-rays (Chandra)

Grey scale – VLA 6 cm radio (Perley & Carilli)

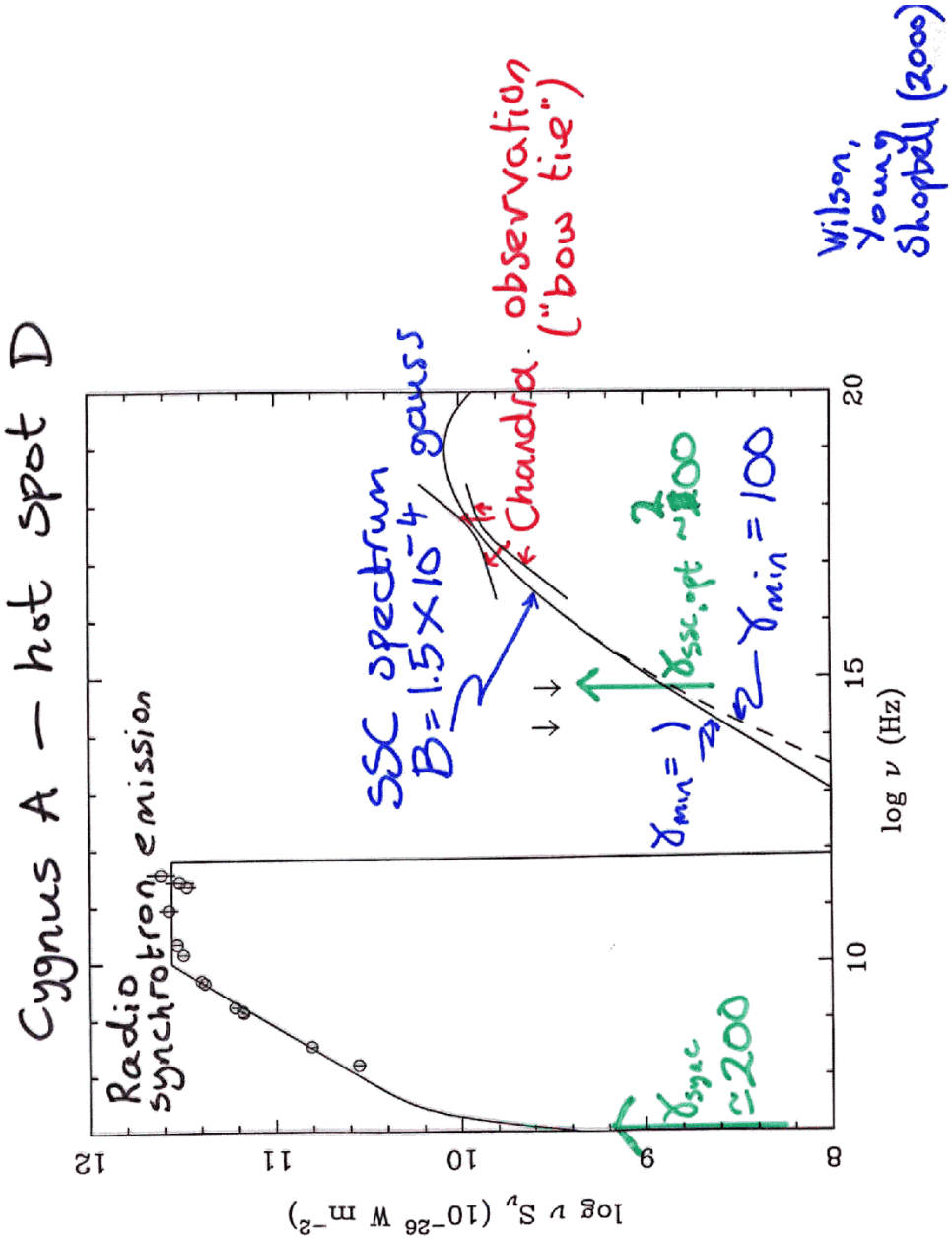

Cygnus A (Hot Spot D)
(Shopbell & ASW)

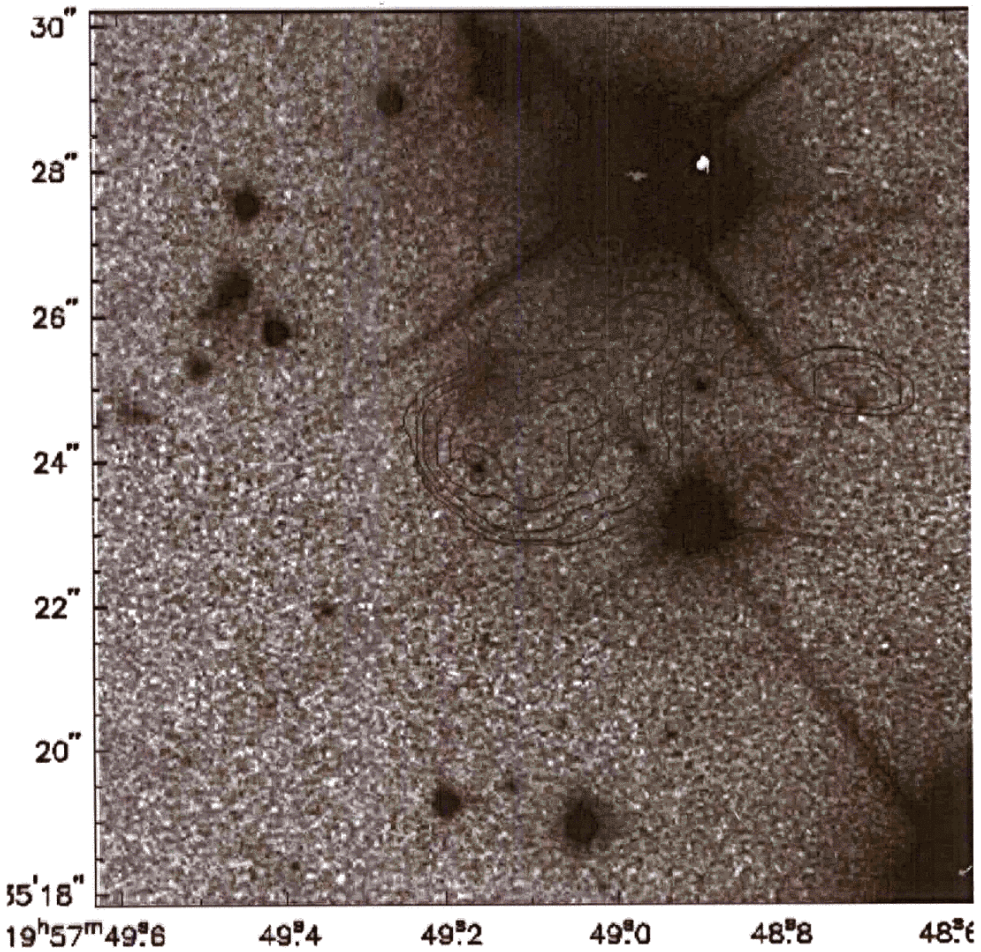

6 cm radio contours (Perley et al.)
on unfiltered HST STIS image

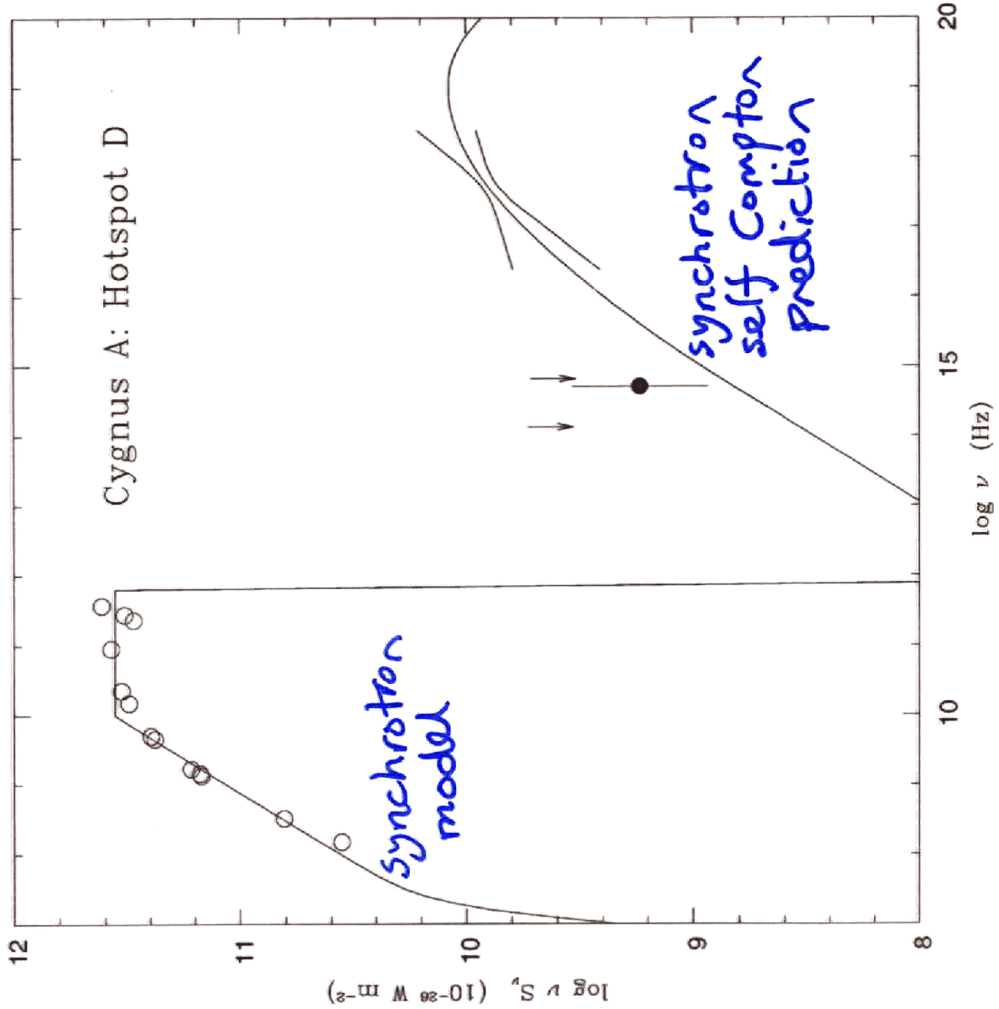

Tavecchio et al. (2000).

Curves for given L_c/L_s

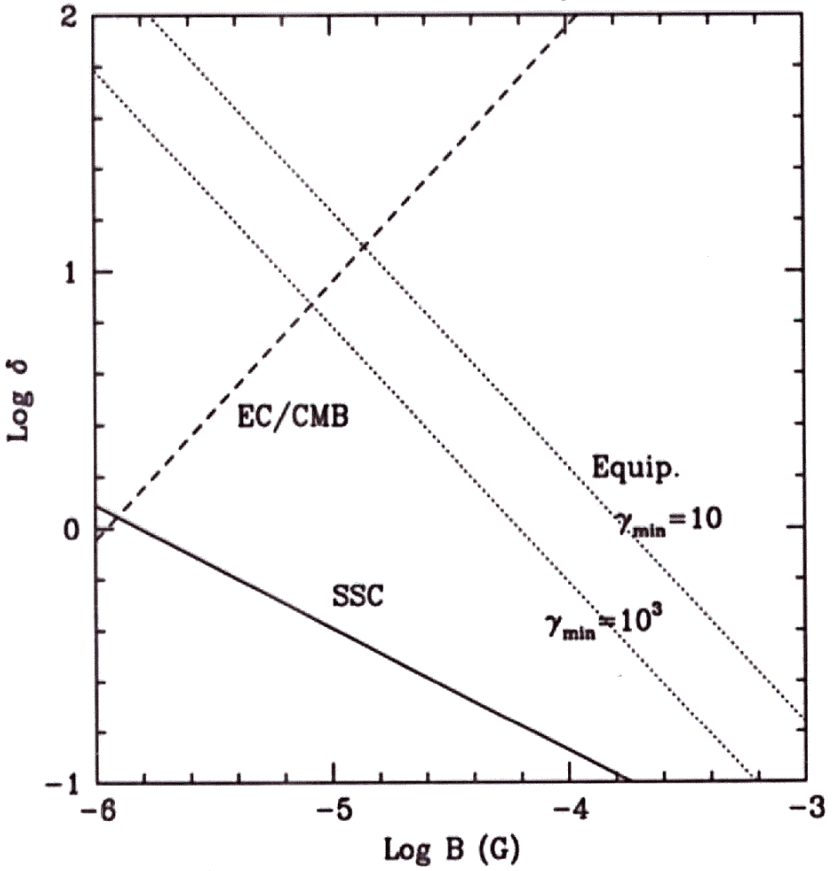

Allowed values of the Doppler factor, δ, and magnetic field for knot WK7.8 of quasar PKS 0637-752

See also Celotti et al. (2001)

Fig. 1 CITED IN TEXT | HI-RES IMAGE (173kb) |

Allowed values of the magnetic field and Doppler beaming factor for knot WK7.8 of PKS 0637-752. *Solid line*: Allowed values of B and δ if the observed X-ray emission is produced by a SSC model. *Dashed line*: Allowed values if the X-rays come from inverse Compton scattering of CMB photons (the EC/CMB model). *Dotted lines*: Allowed values of B and δ under the assumption of equipartition between radiating particles and the magnetic field for two different values of the low-energy cutoff of the electron distribution, $\gamma_{min} = 10$ and $\gamma_{min} = 10^3$. The EC/CMB emission can clearly be consistent with equipartition conditions for moderately large values of the Doppler factor ($\delta \sim 10$), while the SSC case is far from equipartition unless an enormous degree of debeaming is present ($\delta \ll 0.1$). For the calculation, we used the radio flux density at 4.8 GHz and the X-ray flux density at 1 keV reported in Fig. 2.

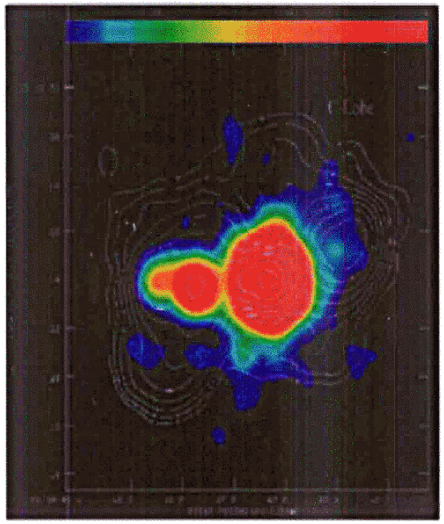

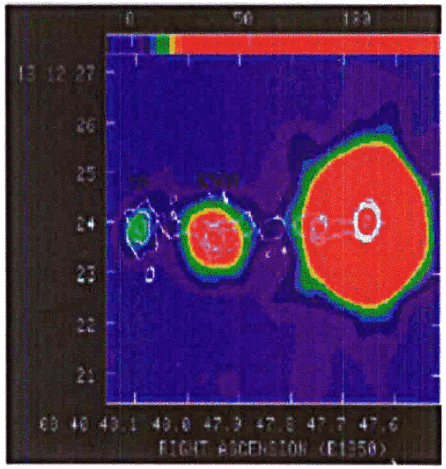

3C 207 (quasar, $z = 0.684$)

Color = X-rays

Contours = radio

Diffuse western X-ray emission argued to be EC scattering of nuclear photons by low energy electrons

Brunetti et al. (2002)

Brunetti et al. (1997)

More distant lobe is brighter in X-rays due to anisotropy of IC radiation.

X-ray jets etc.: statistical results

1) Flat spectrum quasars with radio jets: EC CMB (Marshall et al. 2005)
2) Lobes of $z = 2$ radio galaxies: EC CMB (Overzier et al. 2005)
3) Hot spots of 3C FRII radio gals.
   - Most luminous are SSC in Beq
   - Least luminous – an additional X-ray component (synchrotron?) is present (Hardcastle et al. 2004)
4) kpc scale jets in FRII radio galaxies – EC/CMB and/or synchrotron (Sambruna et al. 2004)

   Jets are still relativistic on kpc scales (as on sub-pc scales) [$\Gamma_{bulk} \sim 5 - 15$]. No deceleration

The M87 Jet in Radio, Optical & X-rays (Perlman & Wilson 2005)

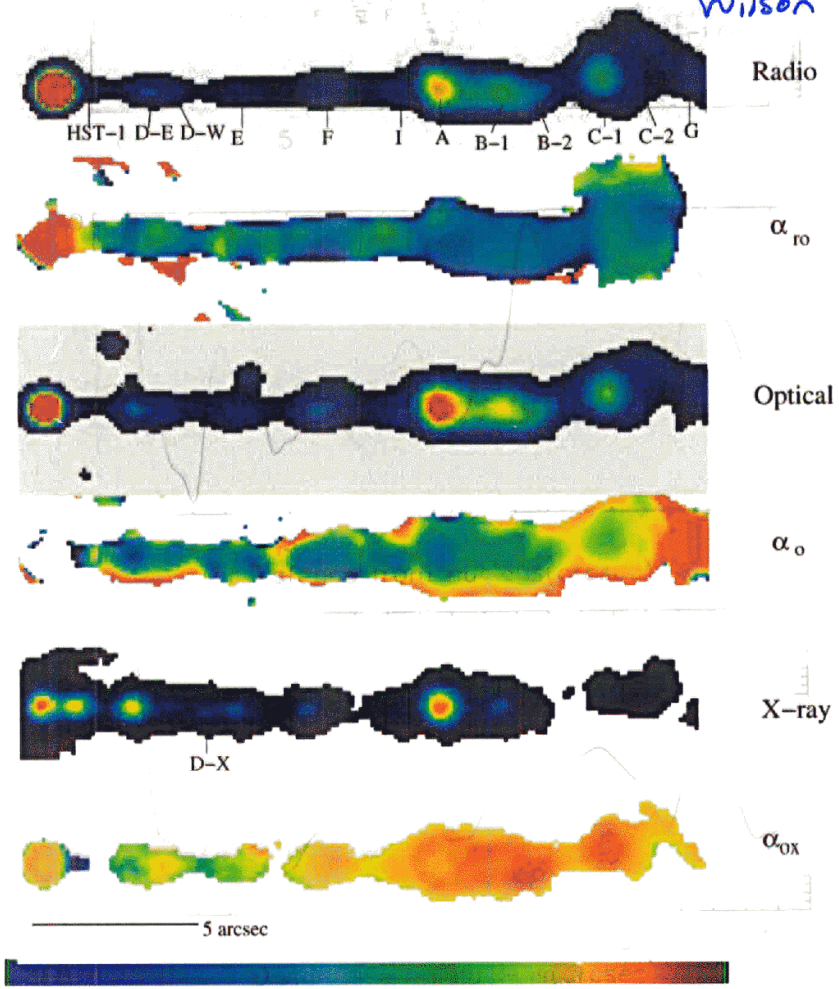

Spectra of knots in jet of M87 (Wilson & Yang 2002)

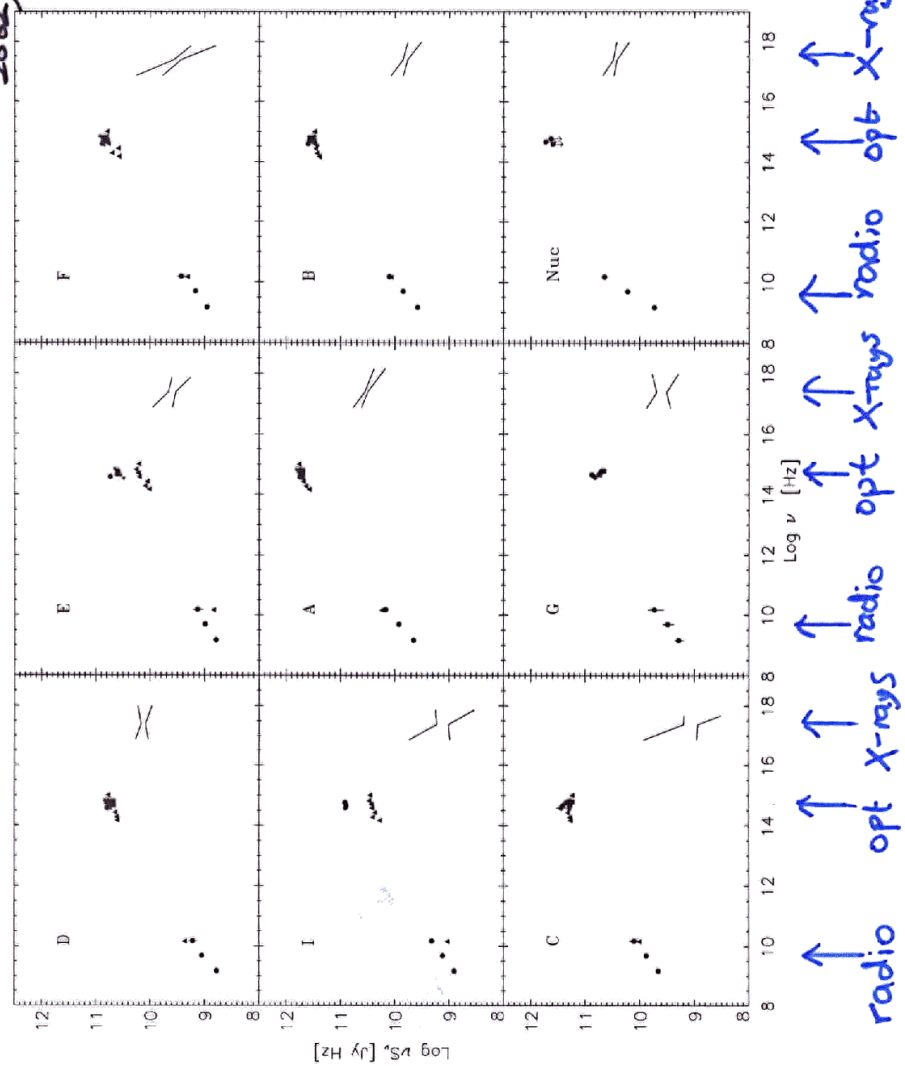

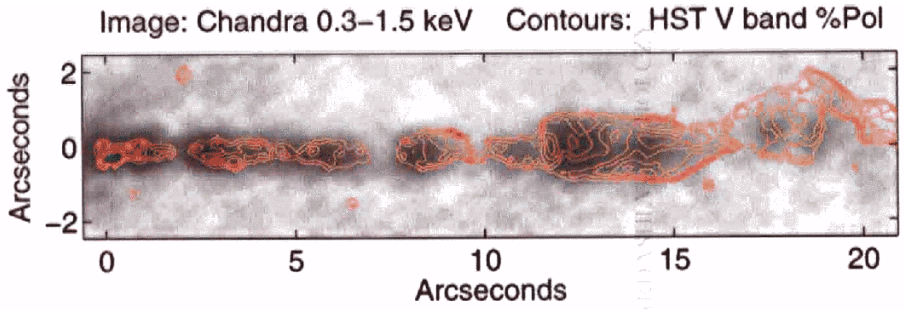

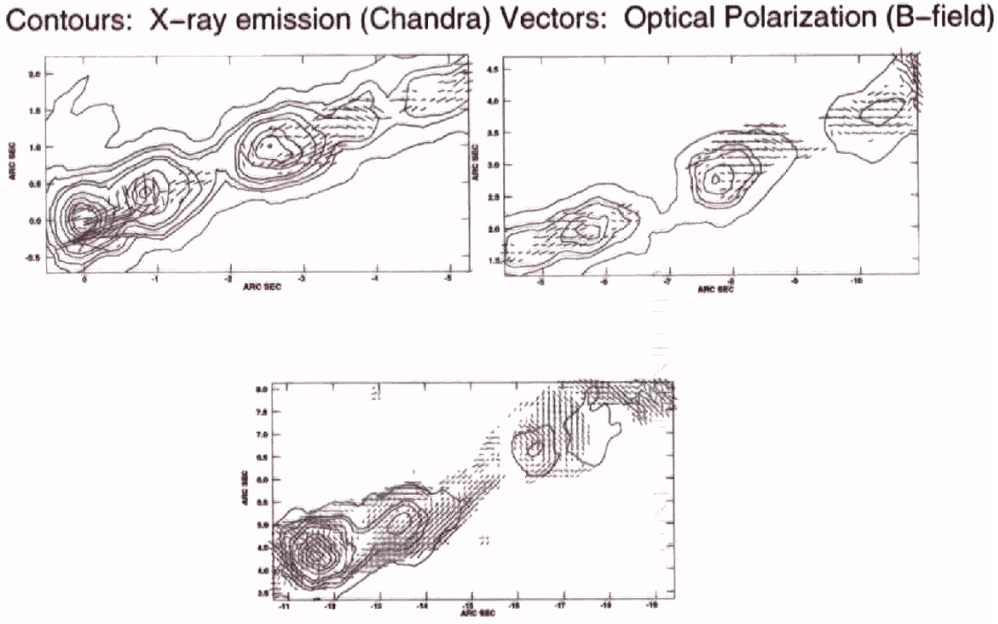

Model of spectral shape of M87 jet

(Perlman & Wilson 2005)

- Assume $N_{inj} \propto E_e^{-\Gamma_{inj}}$, with $\Gamma_{inj} = 2.23$ (as predicted by accel'n in ultrarelativistic shocks – Kirk et al.) at all energies and all locations, up to E_{cutoff}, which varies with position.
- Agrees with $\alpha_r = 0.6$ in ~ all knots.
- Observe $1.0 > \alpha_x - \alpha_r > 0.6$
- Assume particles are accelerated in only f_{acc} (position, energy) x whole volume
- If $f_{acc,r} \simeq 1$, then $f_{acc,o} \sim 1$ and $1 > f_{acc,x} \gtrsim 0.01$
- $f_{acc,x} \propto E_e^{-0.2 \text{ to } -0.4}$

Physical postulate: all shocks accelerate with $\Gamma_{inj} = 2.23$, but E_{cutoff} varies from shock to shock.

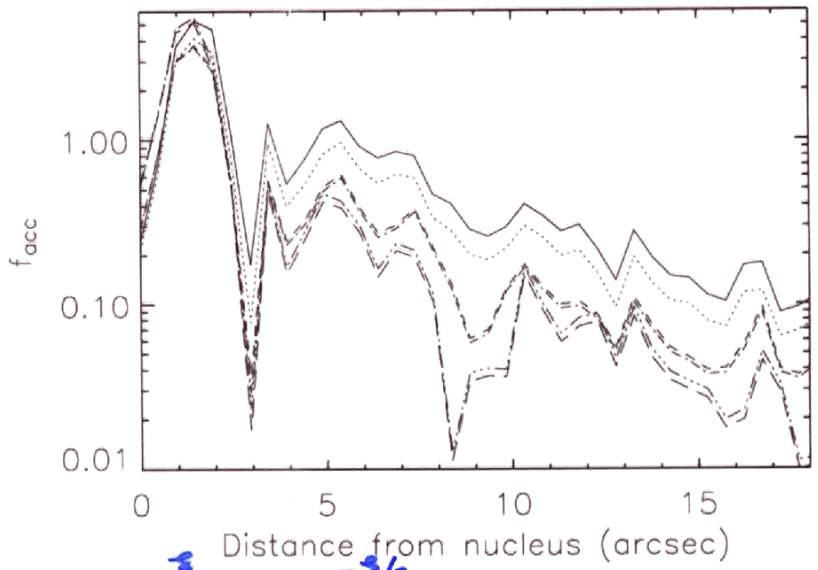

$f_{acc} \propto E_\gamma^{-3} \propto E_e^{-3/2}$

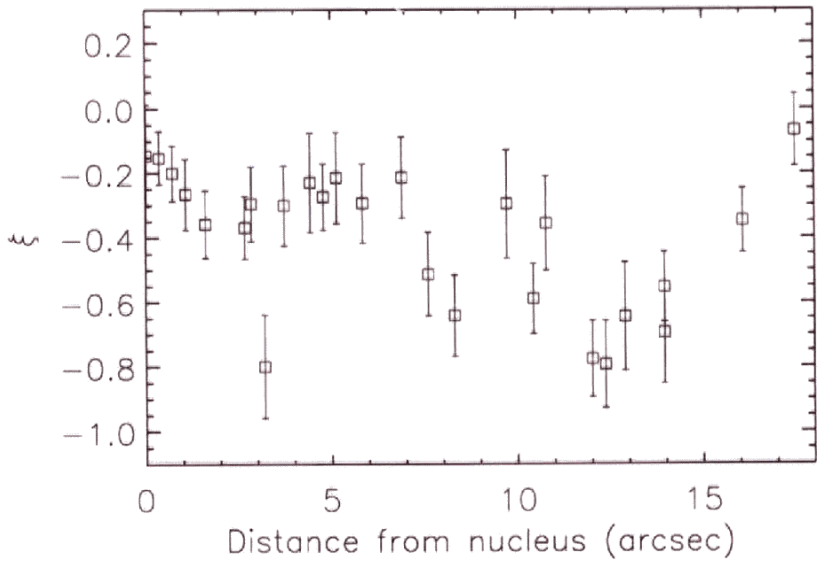

C. G. Mundell et al.

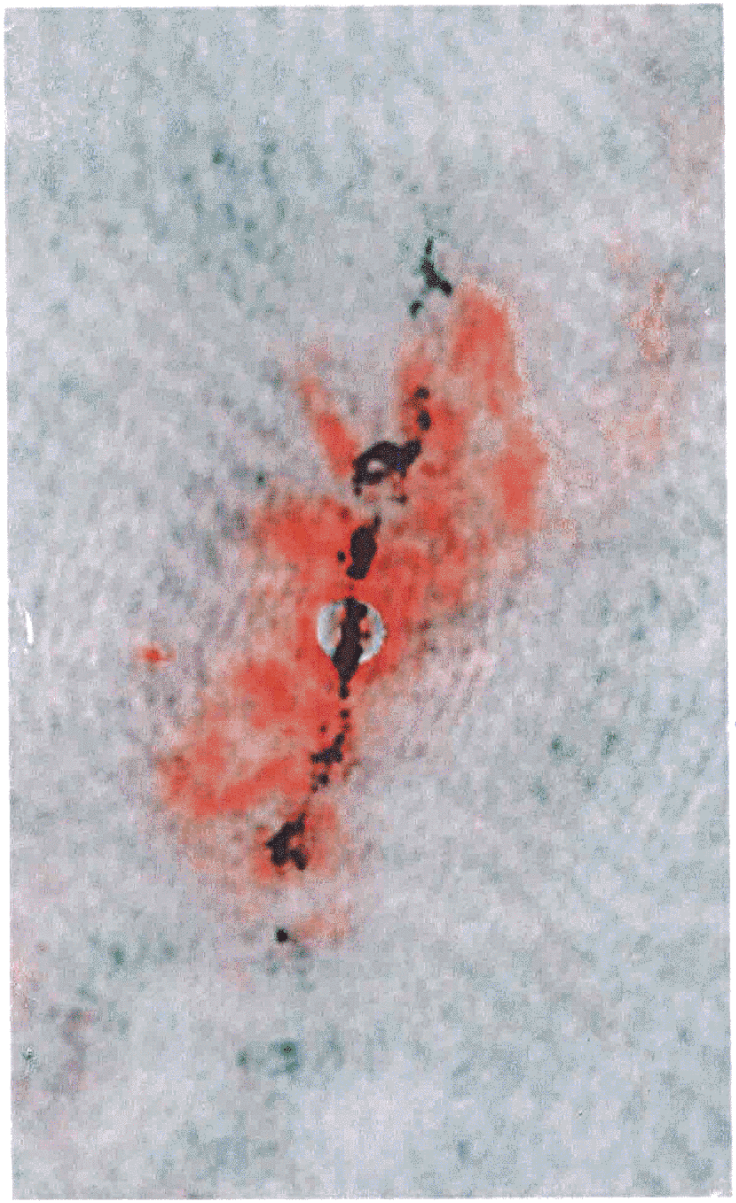

NGC 4151

Black – radio continuum

Red – optical line emission

fg4d.gif (GIF Image, 561x565 pixels) http://www.journals.uchicago.edu/ApJ/journal/issues/ApJ/v516n1/...

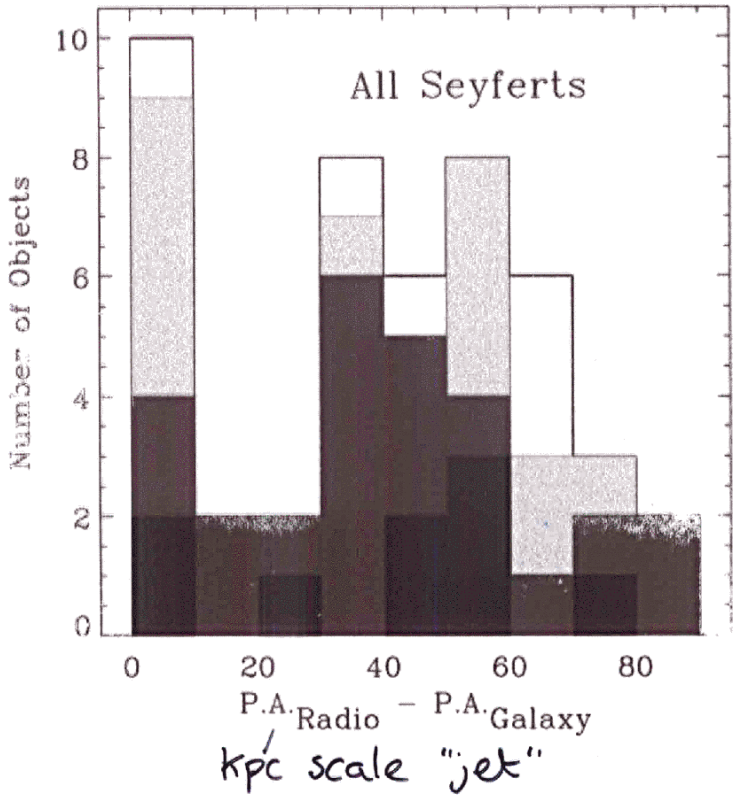

kpc scale "jet"

Nagar & Wilson 1999

Also Clarke et al. 1998
Kinney et al. 2000
Pringle et al.
Schmitt et al.

fg8a.gif (GIF Image, 576x578 pixels) http://www.journals.uchicago.edu/ApJ/journal/issues/ApJ/v516n1/...

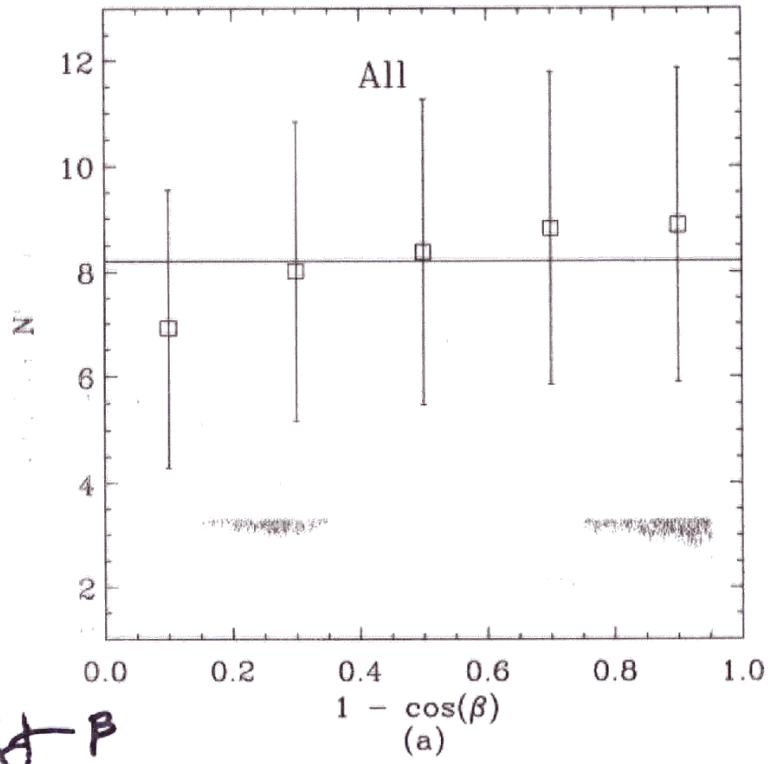

Nagar & Wilson 1999

also Kinney et al. 2000
Clarke et al. 1998

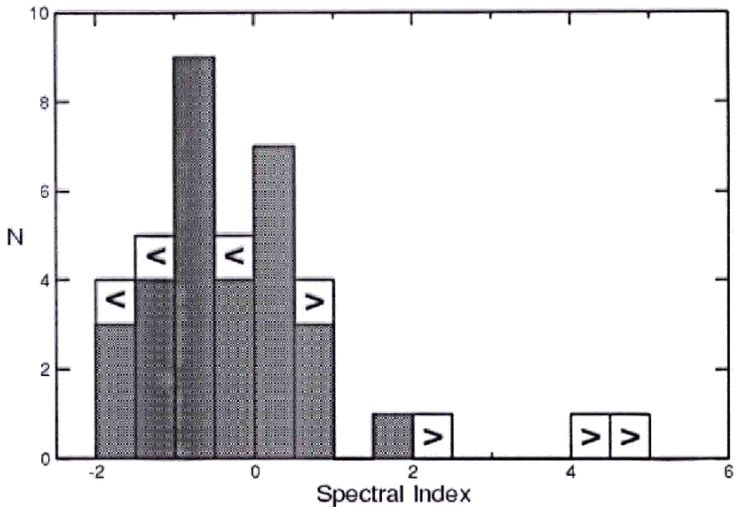

Seyfert jets: pc vs kpc scale orientations

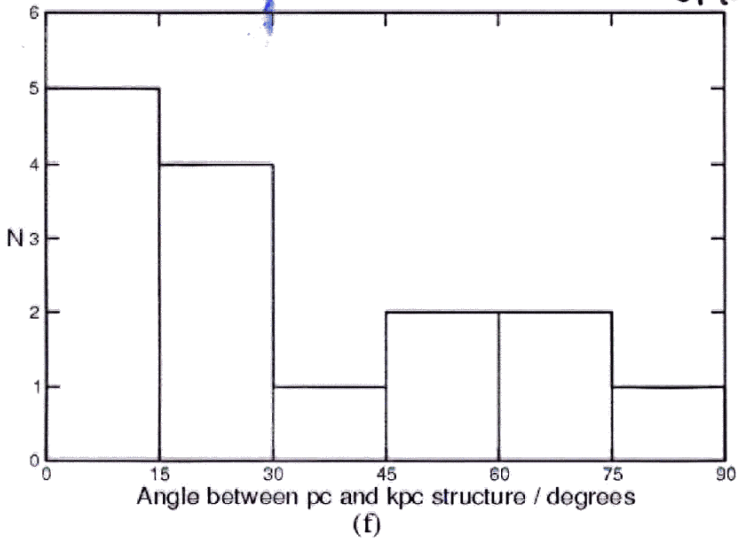

Middelberg et al. 2004

A. L. Roy et al. (2005)

Histogram of apparent velocities

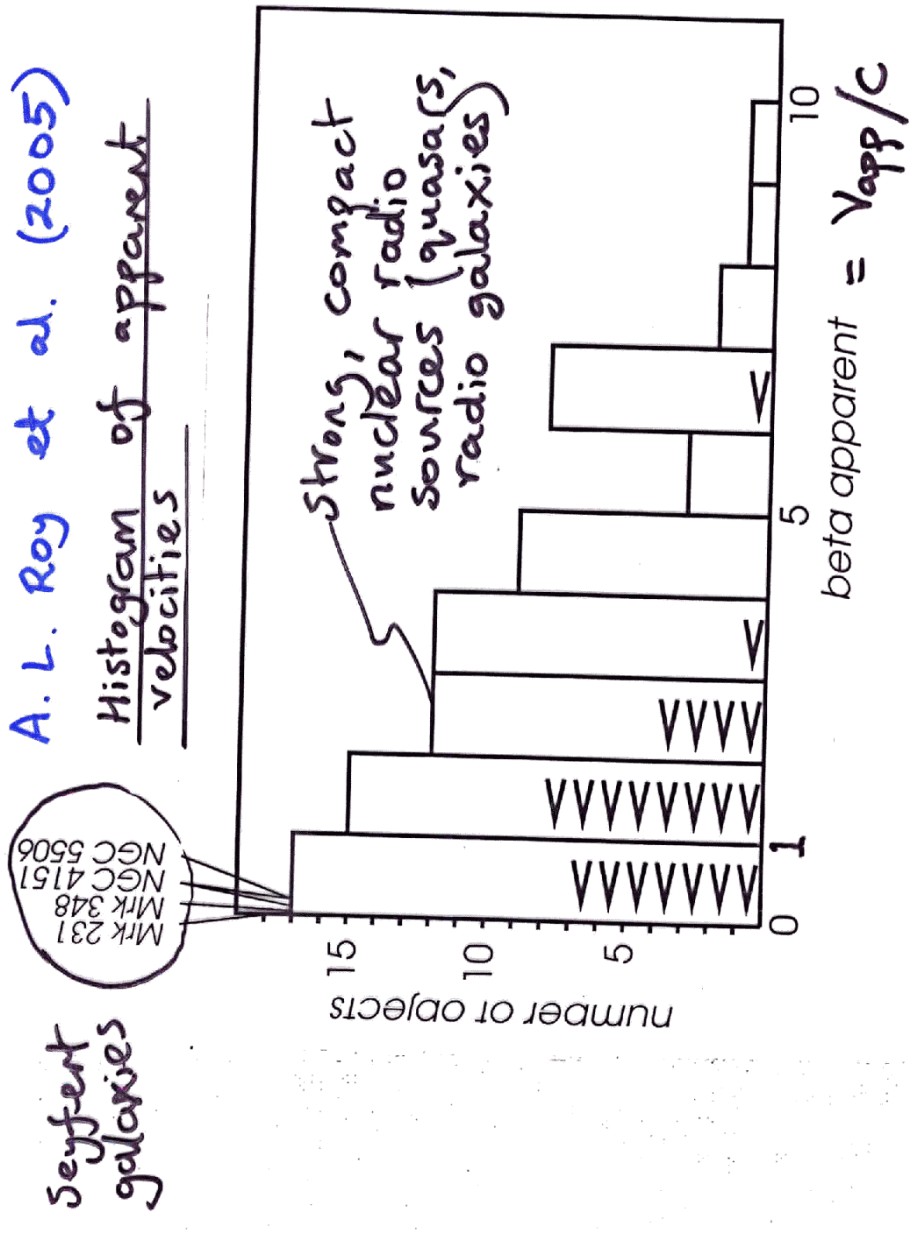

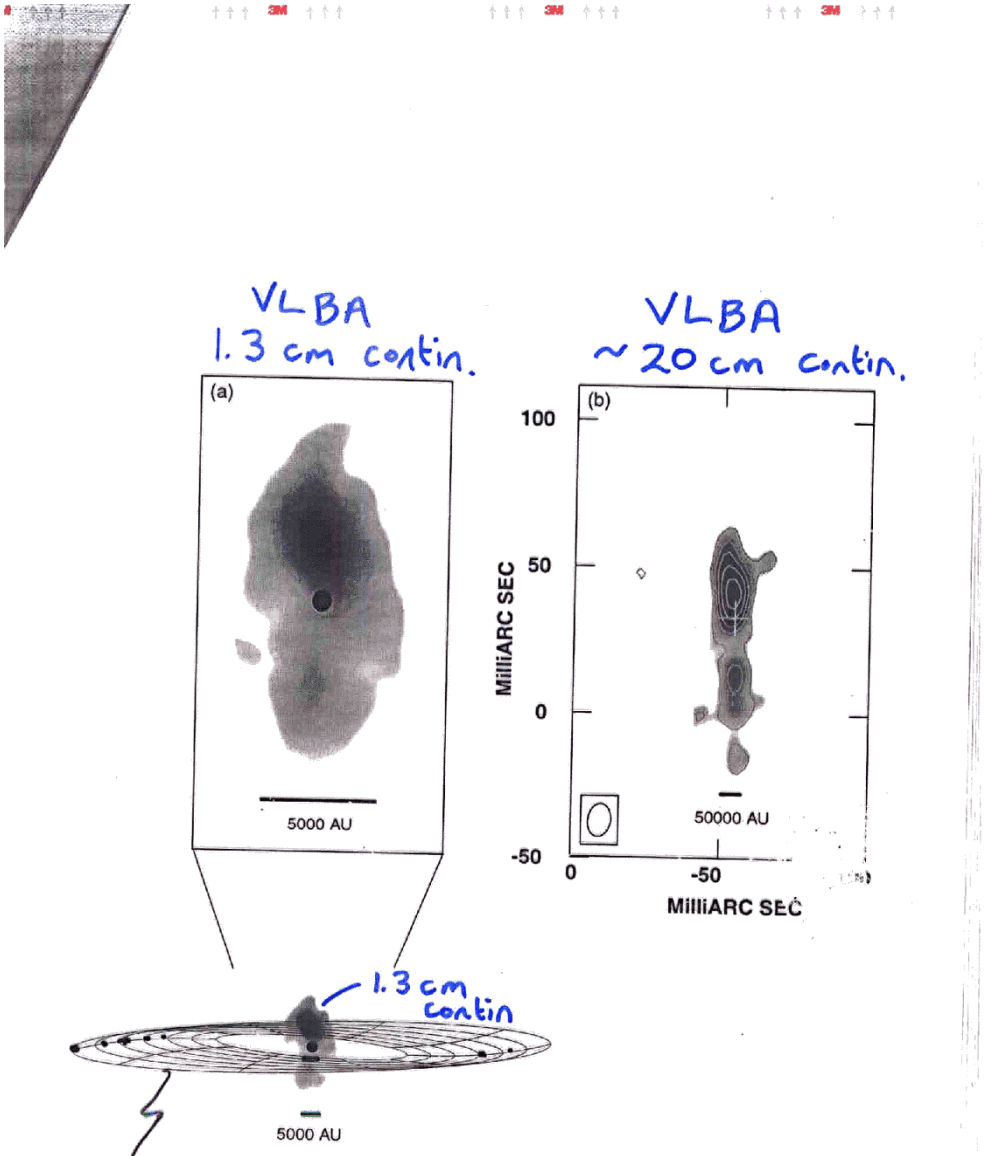

Schematic of H_2O maser disk

Cecil et al. 2000
Herrnstein et al. 1999

Ideas on random orientation of Seyfert jets w.r.t. galaxy disks

Kendall, Magorrian & Pringle (2003):

Minor mergers → multiple nuclear bh coalescences → random orientation of bh spin axis.

Doesn't work for NGC 4258: jet is perp to disk (seen in H_2O masers) on 0.1pc ($\sim 10^{4-5} R_G$) scale.

Papaloizou, Terquem & Lin (1998):

Orbiting companion / minor merger torques gas disk. Good bet.

img58.gif (GIF Image, 815x386 pixels) http://www.edpsciences.org/articles/aa/full/2002/34/aa2300/img58.gif

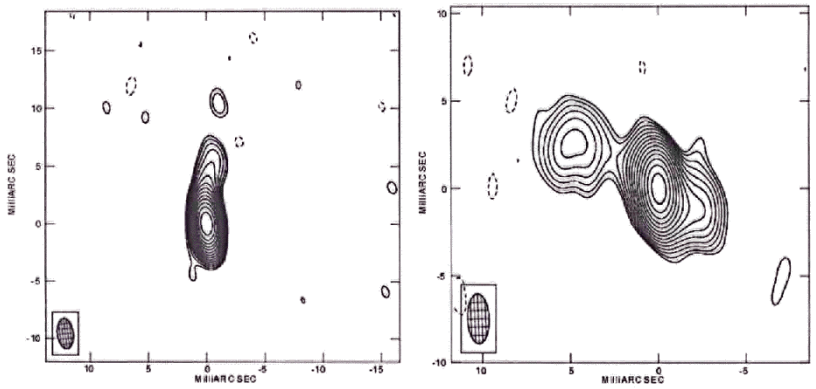

NGC 4374 NGC 4552

VLBI images (~pc-scale) of LLAGN

Nagar et al. 2002

1 of 1 04/29/05 21:40

fg1a.h.gif (GIF Image, 1239x1120 pixels) http://www.journals.uchicago.edu/ApJ/journal/issues/ApJL/v559n...

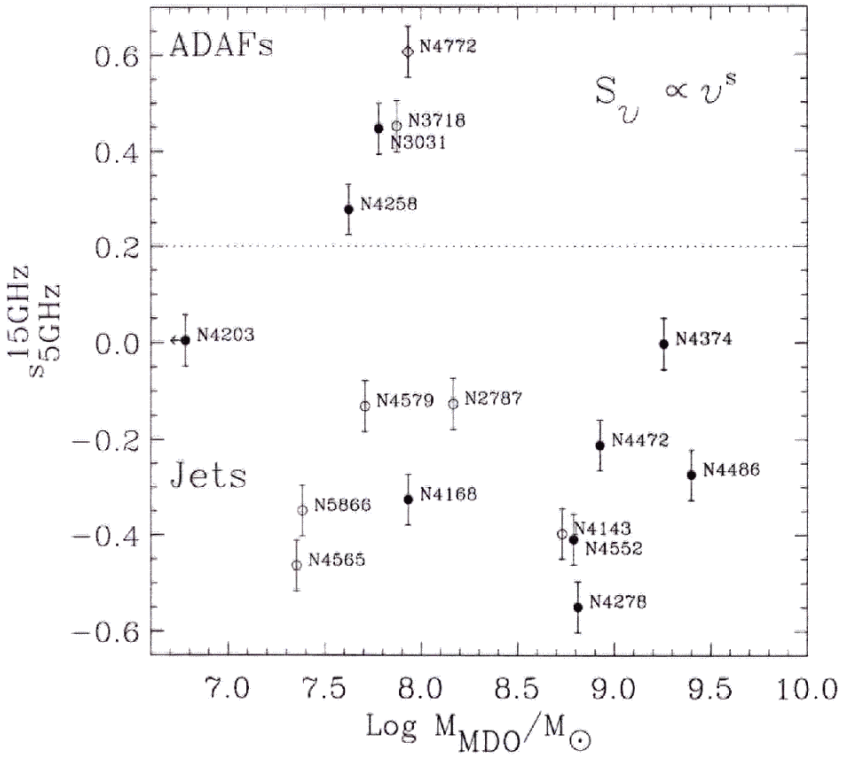

Nagar et al. 2001

(Mahadevan 1997 for expectations of thermal synchrotron emission from ADAFs)

1 of 1 04/29/05 21:29

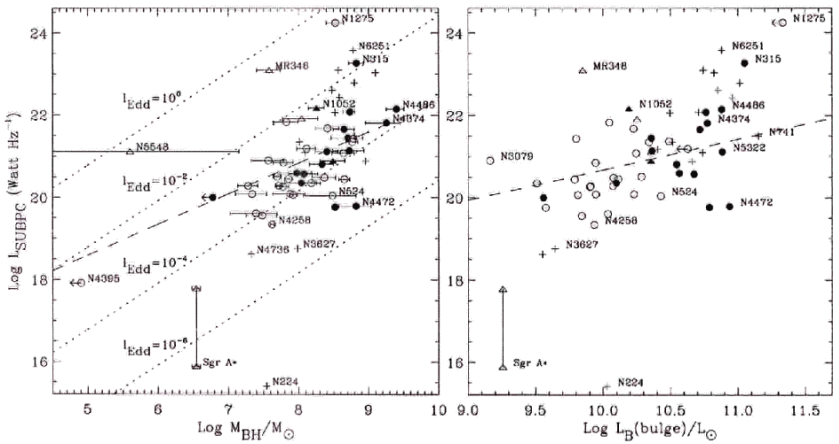

Fig. 4. A plot of sub-parsec radio luminosity versus (left) black hole mass and (right) bulge luminosity of the host galaxy in the B-band. Only radio-detected sources relatively unambiguously identified with the central engine of the AGN (see text) and with radio fluxes measured at resolution better than 1 pc are plotted as circles (Palomar LLAGNs and AGNs) and triangles (other LLAGNs and AGNs). For these, filled symbols are used for elliptical galaxies, and errors in black hole mass are shown (see text). LLAGNs and AGNs (some of which are in the Palomar sample) with radio luminosities measured at resolution between 1 pc and 5 pc are shown as crosses. Two measurements (at different resolutions; Nagar et al., 2002a) are plotted for the Galaxy. The four dotted lines in the left panel represent Eddington ratios (from 10^{-6} to 1) calculated assuming that jet kinetic power dominates the accretion energy output (see Sect. 5.5). The dashed line in the left panel shows a linear fit to the circles and triangles with log $M_{BH} > 10^7$ $M_\odot$; the dashed line in right panel shows a linear fit to the circles and triangles except the Galaxy (see text).

tion of ∼7 mas translates to >1 pc and only some of these FR Is could be included in the figure as crosses. We do not consider other more powerful radio sources (e.g. blazars) to minimize confusion due to relativistic beaming.

A visual inspection of Fig. 4 shows a rough overall correlation between radio luminosity and both black hole mass and galaxy bulge luminosity. The large scatter in both relationships is possibly due to a large range of accretion rates at any given black hole mass (dotted lines in Fig. 4 left), which results in widely different output radio luminosities. Statistical tests[3] from the ASURV package (Lavalley et al., 1992), suggest that both correlations are statistically significant even when the Galaxy and other nuclei with low black hole mass are removed, as detailed below. The radio luminosity and black hole mass correlation has significance 99.95-99.98% when all circles and triangles in Fig. 4 (left panel) are considered. This significance drops only slightly (98.9-99.8%) when the Galaxy and NGC 4395 are not considered, and is still 98.9-99.8% when only nuclei with log $M_{BH} > 10^7$ $M_\odot$ are considered.

[3] Measurement errors were not considered when running the statistical tests.

The correlation between radio luminosity and bulge luminosity has significance 99.3-99.7% when all circles and triangles in Fig. 4 (right panel) are considered. This correlation is still significant (95.6-99.2%) when the Galaxy is not considered. Linear regression analysis by the Buckley James method in ASURV on the circles and triangles in Fig. 4 (not considering the Galaxy in both cases, and using only nuclei with log $M_{BH} > 10^7$ $M_\odot$ in the case of the relation between radio luminosity and M_{BH}) yields:

$$\log(L_{Sub-pc}\,[W/Hz]) = 0.74\,(\pm0.31)\log(L_B(bulge)/L_\odot) + 13.28 \quad (1)$$
$$= 0.75\,(\pm0.26)\log(M_{BH}/M_\odot) + 14.84$$

These two relations are plotted with dashed lines in Fig. 4.

The relation between radio luminosity and black hole mass has been discussed by several authors, with conflicting results. For example, Franceschini et al. (1998) claimed a correlation with a much steeper slope based on a small number of objects, while Ho (2002) and Woo & Urry (2002) found no correlation for larger samples of AGNs and LLAGNs. We emphasize that our results and those of Ho (2002) and Woo & Urry (2002) are not contradic-

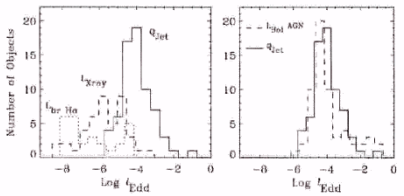

Fig. 7. A comparison of the kinetic and radiated accretion power outputs as a fraction of $L_{Eddington}$ in four energetically important wavebands. In both panels the histograms are offset by 0.1 in x for clarity. **Left:** histograms of the broad Hα luminosity (dotted line), hard X-ray luminosity (2–10 keV; dashed line), and minimum jet power (Q_{jet}; solid line) for all broad line nuclei, all hard X-ray detected nuclei, and all radio detected nuclei, among the LLAGNs and AGNs of the Palomar Sample, respectively. **Right:** histograms of the minimum jet power (Q_{jet}; solid line) and radiated bolometric luminosity (derived from the [O III] luminosity, see text; dashed line) for the radio detected nuclei in the LLAGNs and AGNs of the Palomar Sample.

5.5.1. Jet Power Domination in Palomar LLAGNs

With an estimated black hole mass and an emitted luminosity, one can estimate the Eddington ratio, i.e. $l_{Edd} = L_{Emitted}/L_{Eddington}$. Previous calculations of l_{Edd} for LLAGNs have considered only the radiated component of $L_{Emitted}$. Since LLAGNs lack a 'big blue bump', the X-ray emission has been thought to dominate the bolometric luminosity (Ho, 1999). With most LLAGNs having hard X-ray luminosities of only $\sim 10^{40}$ erg s^{-1} or lower, the accretion is inferred to be highly sub-Eddington (Ho et al., 2001; Terashima & Wilson, 2003; Filho et al., 2004).

If, as justified above, the compact radio nuclei and sub-parsec jets represent emission from the base of a relativistic jet launched close to the black hole, then the kinetic energy in the jet can be quite high. Equation 20 of Falcke & Biermann (1999) - assuming an average inclination of 45° - can be used to obtain 'minimum jet powers' (Q_{jet}) of $10^{40} - 10^{45}$ erg s^{-1} (Fig. 6, left panel) from the 15 GHz peak VLA flux of radio detected LLAGNs. For LLAGNs with both hard X-ray and radio luminosity available, this jet power greatly exceeds the radiated X-ray luminosity (Fig. 6, right panel). Since the bolometric luminosity (L_{Bol}) in electromagnetic radiation is estimated to be only $\sim 3 - 15 \times L_{0.5-10\,keV}$ for LLAGNs (Ho, 1999), this suggests that the accretion power output is dominated by the jet power. This domination of jet power over X-ray emission is analogous to the situations for ∼10-15 $M_\odot$ black holes in Galactic X-ray binary systems (Fender, Gallo, & Jonker, 2003) and for powerful radio galaxies (e.g. Celotti & Fabian, 1993; Owen, Eilek, & Kassim, 2000).

To expand on this issue, we compare the estimated minimum jet power to the observed hard X-ray luminosity and emission-line luminosities for the Palomar sample LLAGNs. Clearly (Fig. 7, left) the minimum jet power is significantly larger than the measured hard X-ray luminosity (as noted above) and the luminosity in broad Hα. On the other hand, if the radiated bolometric luminosity is estimated from the [O III] luminosity - from the empirical result that the spectral energy density of type 1 AGNs typically shows $L_{Bol} = 3500 \times L_{[OIII]}$ (Heckman et al., 2004, see also next Sect.) - then LLAGNs show similar distributions of minimum jet power and radiated bolometric luminosity (Fig. 7, right).

5.5.2. A Common Jet-Power Scaling for LLAGNs and Powerful AGNs

The radio detected LLAGNs in the Palomar sample (circles; Fig. 8) fall nicely at the low luminosity end of the correlation between jet kinetic power and total emission line luminosity from the narrow line region (NLR) for more powerful FR I and FR II galaxies. This figure includes FR I and FR II radio galaxies (slanted crosses; in these the jet kinetic power is estimated from lobe-feeding energy arguments; Rawlings & Saunders, 1991) and other powerful radio sources (including BL Lacs, quasars, and radio galaxies) with parsec-scale jets (crosses; in these the bulk kinetic energy in the jet was estimated using a self-Compton synchrotron model applied to the parsec-scale jet; Celotti & Fabian, 1993). We estimated the NLR luminosity for the Palomar LLAGNs and AGNs following Celotti & Fabian (1993):

$L_{NLR} = 3 \times (3\,L_{[OII]\lambda3727} + 1.5\,L_{[OIII]\lambda5007})$

with $L_{[OII]\lambda3727}$ estimated as $0.25\times L_{[OIII]\lambda5007}$ for Seyferts and $3\times L_{[OIII]\lambda5007}$ for LINERs and transition nuclei. The Palomar [O III] luminosities were measured in a $2''\times4''$ nuclear aperture (Ho et al., 1997a); these values closely approximate the total NLR luminosity in most nuclei except a handful, e.g. NGC 4151, which have more extended NLRs.

5.5.3. LLAGN Jet-Power and Global Energetics

The energetics of the jet are also important in the context of so called cooling flows and in regulating the feedback between galaxy growth and black hole growth. For example, in many clusters the central cD galaxy has an FR I radio morphology, with the radio jet playing an important role in the above issues and in the global energetics of the cluster gas (Owen, Eilek, & Kassim, 2000; Binney, 2004b; Ostriker & Ciotti, 2004). A comparison of the jet kinetic power with the power injected into the ISM by supernovae types I and II in the host galaxies is shown in Fig. 9 for the radio detected Palomar LLAGNs/AGNs. The supernova rates (as a function of galaxy morphological type) are taken from the "Case B" values in Table 6 of van den Bergh & McClure (1994), e.g. 0.25 SNu for E and

S0 galaxies (all from SN type Ia), where 1 SNu = 1 SN per century per $10^{10}(L_B/L_\odot)$. The total SN rate is slightly higher in later type galaxies due to the contribution of SN type II. Values of $L_B/L_\odot$ were taken from Ho et al. (1997a) and each supernova is assumed to inject 10^{51} erg of kinetic energy into the ISM (e.g. Binney & Tremaine, 1987; Pellegrini & Ciotti, 1998). The jet power is clearly the major player in the nuclear energetics not only because it exceeds the total SN kinetic power in almost all cases, but also because its nuclear origin allows a closer 'feedback' to the accretion inflow. A significant fraction of the jet energy is potentially deposited in the central parsecs, especially in LLAGNs which show pc-scale (usually bent) jets but no larger scale jets (Sect. 5.4); such deposition of jet power can considerably slow down or balance any cooling flow or other inflow in the inner parsecs and thus ultimately help 'starve' the accretion disk (e.g. Di Matteo et al., 2001). Additionally, LLAGNs with kpc-scale jets inject significant energy into the inter-galactic medium (IGM), and work against any cooling flow (see e.g. Pellegrini & Ciotti, 1998). The most recent of such 'feedback' analyses (Binney, 2004b) does take into account the jet power, though for the more powerful FR I type jets in cD galaxies. Our results show that their models can be applied, at least qualitatively, to LLAGNs.

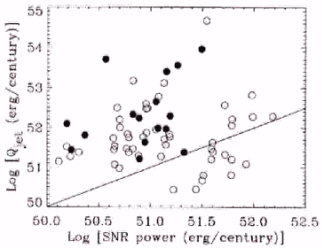

Fig. 9. A comparison of the 'minimum jet power' (Q_{jet}) and the kinetic energy injected into the ISM by supernovae type I and II for the radio detected Palomar LLAGNs and AGNs. Filled circles are used for elliptical galaxies. The solid line shows the line of equality.

In summary, Eddington ratios, l_{Edd}, calculated from hard X-ray luminosities heavily underestimate the true accretion power output in LLAGNs. This finding is in line with that for more powerful radio galaxies, where the jet kinetic power is two to five orders of magnitude larger than the radiated radio luminosity, and often significantly larger than the total radiated bolometric luminosity (Celotti & Fabian, 1993; Owen, Eilek, & Kassim, 2000). Using $L_{Bol} = 3500\ L_{[OIII]}$ or $L_{Bol} = Q_{jet}$ yields similar distributions of L_{Bol}. This, and the scaling between L_{NLR} and Q_{jet}, argues for a common central engine in all AGNs from LLAGNs to powerful FR IIs, but with the caveat that the [O III] luminosity in LLAGNs is potentially contaminated by non accretion related processes. Finally, the jet is potentially a significant (maybe even dominant) source of heating in the galaxy. If the jet is disrupted in the inner parsecs, then the jet power could play a role in slowing any cooling flow or other accretion inflow on parsec-scales, thus starving the accretion disk.

5.6. The Eddington Ratio

In the previous section we showed that the accretion energy output in LLAGNs with radio nuclei is dominated by the jet power, and is of the order of $l_{Edd} = 10^{-6}$ to 10^{-2}. Here we look at the dependence of this jet-power-derived l_{Edd} on other quantities.

Heckman et al. (2004) have investigated black hole and galaxy growth using 23,000 type 2 AGNs from the Sloan Digital Sky Survey (SDSS). They use σ_c to estimate black hole mass, and $L_{Bol} = 3500\ L_{[OIII]}$. They find that most present-day accretion occurs onto black holes with masses $< 3 \times 10^7\ M_\odot$, and that most black hole growth takes place in systems with accretion rate less than one fifth of the Eddington rate. It is interesting to apply their analysis to the Palomar LLAGNs since these objects have emission-line luminosities typically ten to a hundred times fainter than the SDSS AGNs. The Palomar LLAGNs show a different behavior to the SDSS AGNs: the numerous Palomar LLAGNs with low black hole masses are accreting a similar mass per year as the fewer Palomar LLAGNs and Palomar AGNs at higher radio luminosity. This is true whether the accretion rate is calculated from the [O III] luminosity, as in Heckman et al. (2004), or from Q_{jet} (e.g. Fig. 5, upper x-axis).

The Palomar sample ellipticals (filled symbols in Fig. 10) show a strong correlation between Eddington ratio, l_{Edd} (calculated assuming the jet power dominates the accretion energy output) and all of emission-line luminosity, radio luminosity, and the ratio of radio luminosity to emission line luminosity. Among the non-elliptical nuclei (open symbols in Fig. 10), Seyfert nuclei (triangles) display higher Eddington ratios than LINERs (circles), even though the distribution of radio luminosities (from which Q_{jet} is calculated) is similar for the two classes. This is most clearly noticeable in Fig. 10c.

5.7. Discovery of LLAGNs: A Comparison of Radio, Optical, and X-ray Methods

The current study and sample allows a comparison of the relative success of deep optical spectroscopy, high resolution radio imaging, and (to some extent) hard X-ray imaging, in identifying low-luminosity accreting black holes. Such a comparison is specially relevant in view of the several hundred thousand AGNs and LLAGNs being identified by current large surveys out to $z \sim 6$. We consider